JOC The Journal of Organic Chemistry

Featured Article

pubs.acs.org/joc

# Computational Study and Kinetic Analysis of the Aminolysis of Thiolactones

Gilles B. Desmet,[†] Dagmar R. D'hooge,[†] Maarten K. Sabbe,[†] Guy B. Marin,[†] Filip E. Du Prez,[‡] Pieter Espeel,*[,‡] and Marie-Françoise Reyniers*[,†]

[†]Laboratory for Chemical Technology, Ghent University, Technologiepark 914, B-9052 Gent, Belgium

[‡]Polymer Chemistry Research Group, Ghent University, Krijgslaan 281 S4-bis, B-9000 Gent, Belgium

Supporting Information

**ABSTRACT:** The aminolysis of three differently $\alpha$-substituted $\gamma$-thiolactones ($C_4H_5OSX$, X = H, $NH_2$, and NH(CO)-$CH_3$) is modeled based on CBS-QB3 calculated free energies corrected for solvation using COSMO-RS. For the first time, quantitative kinetic and thermodynamic data are provided for the concerted path and the stepwise path over a neutral tetrahedral intermediate. These paths can take place via an unassisted, an amine-assisted, or a thiol-assisted mechanism. Amine assistance lowers the free energy barriers along both paths, while thiol assistance only lowers the formation of the neutral tetrahedral intermediate. Based on the ab initio calculated rate coefficients, a kinetic model is constructed that is able to reliably describe experimental observations for the aminolysis of *N*-acetyl-DL-homocysteine thiolactone with *n*-butylamine in THF and $CHCl_3$. Reaction path analysis shows that for all conditions relevant for applications in polymer synthesis and postpolymer modification, an assisted stepwise mechanism is operative in which the formation of the neutral tetrahedral intermediate is rate-determining and which is mainly amine-assisted at low conversions and thiol-assisted at high conversions.

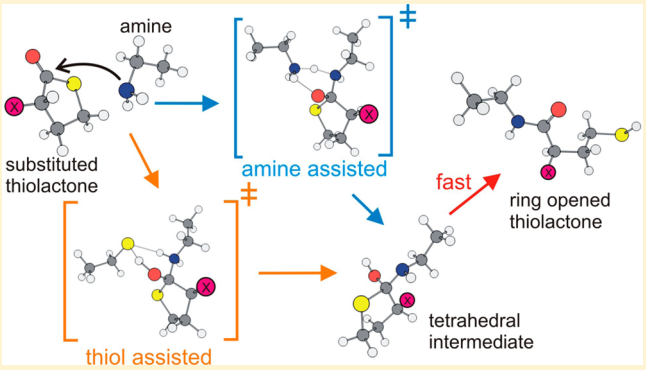


## INTRODUCTION

The aminolysis of $\gamma$-thiolactones, a class of five-membered cyclic thioesters, has witnessed an increasing interest in recent years in the fields of (bio)medicine,[1−6] drug design,[7] peptide science,[8,9] and polymer science.[10−25] The biomedical importance of thiolactones is predominantly due to the homocysteinilation of proteins, which is an important risk factor in the study of vascular diseases, such as atherosclerosis.[26] Homocysteinilation occurs when homocysteine thiolactone, a cyclic thioester of the nonprotein $\alpha$-amino acid homocysteine, reacts with the $\varepsilon$-amine group of lysine residues. This biochemical reaction has been mimicked in many different fields. One of the first applications was the introduction of sulfhydryl groups in natural proteins in peptide synthesis.[8,9] More recent applications are found in synthetic polymer science, in which the aminolysis of thiolactones is used for the in situ formation of thiols, which opens a realm of possible thiol-based polymer modifications.[11,16−18] Thiol chemistry is efficient, fast, and capable of being conducted under mild conditions in different environments[27] and is therefore highly applicable in polymer science, as evidenced by its successful application for the functionalization of a variety of polymers to prepare, for example, thin films, hydrogels, cross-linked networks, self-healing coatings, patterned surfaces, and biomaterials.[28−33] Thiols can react with enes, ynes, acrylates, and epoxy functions.[34−39] For example, one-pot aminolysis of a thiolactone followed by a thiol−ene reaction is known as *amine−thiol−ene conjugation*.[11,16,17] In this approach, thiolactones are effectively used as precursor molecules to circumvent inherent complications with the direct use of thiols, due to their high reactivity, bad odor, and limited commercial availability.

Notwithstanding the numerous applications of thiolactone aminolysis, the mechanistic details of this reaction have not been fully investigated, although an adequate description of the aminolysis of thiolactones, in reaction conditions relevant for applications in polymer chemistry and material science, would be quite relevant for future developments. Garel and Tawfik[1] have investigated the mechanism of both the hydrolysis and the aminolysis of homocysteine thiolactone in terms of pH dependency, as their main perspective was to investigate the reactivity toward various protein amino groups because of the biomedical importance of this reaction. However, a reaction mechanism in terms of elementary reaction steps has, to the best of our knowledge, not been established before. Fortunately, a number of reactions which can be expected to share many characteristics with the aminolysis of thiolactones, such as the aminolysis of esters,[40−47] lactones,[48] phosphono-

**Received:** June 25, 2015
**Published:** August 17, 2015





DOI: 10.1021/acs.joc.5b01446
J. Org. Chem. 2015, 80, 8520−8529

thiolates,[49] oxazolinones,[50] anhydrides,[51] and thioesters,[52,53] have already been extensively studied. Based on these studies, a reaction scheme consisting of three different paths can be put forward for the aminolysis of γ-thiolactones with a primary amine, which is depicted in Figure 1. In the first path (top),

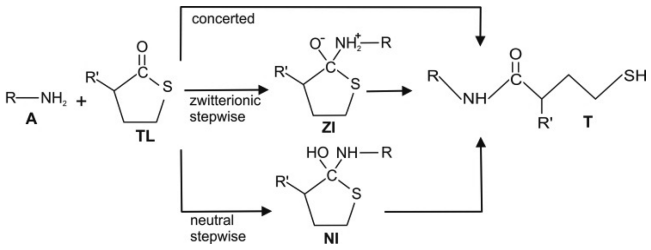


**Figure 1.** Possible reaction paths for the aminolysis of a thiolactone (TL) with a primary amine (A), based on analogous aminolysis reactions of 2-benzoxazolinone,[50] oxoesters, and thioesters:[53] concerted, stepwise via a zwitterionic intermediate (ZI), or stepwise via a neutral intermediate (NI).

both the formation of the N−C bond and the cleavage of the C−S bond occur simultaneously with a proton transfer from the amine nitrogen to the sulfur. The second path (middle) passes over a tetrahedral zwitterionic intermediate (ZI), resulting from the nucleophilic attack of the amine nitrogen at the carbonyl carbon of the thiolactone. In the third path (bottom), first the formation of the N−C bond and a proton transfer from the amine nitrogen to the carbonyl oxygen take place, forming a neutral tetrahedral intermediate (NI), which then reacts further to the thiol product via cleavage of the C−S bond and proton transfer from the hydroxyl oxygen to the sulfur.

It should be noted that most computational studies reported so far only support the concerted and the neutral stepwise mechanism. In one study,[51] computational evidence for the existence of a zwitterionic intermediate in the aminolysis of anhydrides has been mentioned, but the zwitterionic intermediate could only be located as a stable minimum on the potential energy surface if a polarizable continuum model for water is considered during the geometry optimization. However, for benzoxazolinones, a similar approach did not result in stable zwitterionic geometries,[50] and neither for esters nor thioesters have such zwitterionic intermediates been reported.

In contrast to mechanisms involving anionic nucleophiles, aminolysis reactions are considerably more complex since proton transfer needs to occur at a given stage in the reaction.[53] Unfavorable geometries for proton transfer are found to form a major contribution to the energy barrier.[43] Notably, for esters, transition states in which a second amine molecule is assisting in the proton transfer are distinctively lower in energy.[44] In these termolecular transition states, the assisting amine first accepts a proton from the nucleophilic amine before donating one of his own to the oxygen, all in a synchronized movement. Experimental investigations indeed show that the observed rate for the aminolysis reactions of esters in aprotic solvents also shows a quadratic dependence on the amine concentration (1):[41]

$$r_{obs} = k_1[\text{amine}][\text{ester}] + k_2[\text{amine}]^2[\text{ester}] \quad (1)$$

where $k_1$ and $k_2$ are the observed apparent rate coefficients.

Additionally, for the aminolysis of anhydrides, catalysis by an acid molecule has been discussed,[51] leading to an autocatalytic reaction. The situation becomes even more complex in protic solvents, such as water. The solvent itself can then assist in the formation of the transition state, significantly lowering its energy,[53] but additionally, the pH of the solution can also have an influence on the observed rate.[1,52,54]

The present investigation is a combined experimental and theoretical study of the aminolysis of saturated γ-thiolactones in aprotic solvents. For the computational study, three differently substituted thiolactones (Figure 2) are selected as model compounds.

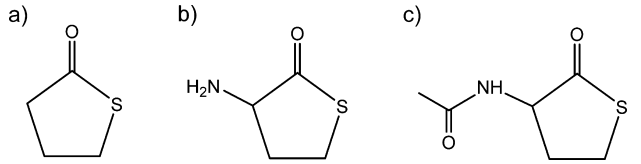


**Figure 2.** Chemical structures of the thiolactones investigated in this study: (a) γ-thiobutyrolactone (γTBL), (b) homocysteine thiolactone (tHcy), and (c) *N*-acetyl-DL-homocysteine thiolactone (ActHcy).

Tetrahydrofuran (THF) and chloroform ($CHCl_3$) are chosen as aprotic solvents, as these are also typically used in polymeric applications, in general, and in amine−thiol−ene conjugation, in particular.[11] The three aforementioned paths, that is, concerted, zwitterionic stepwise, and neutral stepwise, are considered, as well as the possible assistance by stable nucleophilic species present in the reaction mixture, such as amines or thiols. High level computational methods (CBS-QB3[55] and COSMO-RS[56]) are used to investigate the different mechanisms and to obtain the relevant thermodynamic and kinetic parameters, using ethylamine as a model compound for the nucleophilic agent and ethanethiol as a model compound for the ring-opened thiolactone in the thiol-assisted mechanisms. Next, a kinetic model is constructed, based on the computationally obtained rate coefficients. The kinetic model is validated by comparison with experimental data for the aminolysis of the practically most relevant thiolactone, ActHcy, with *n*-butylamine in THF and $CHCl_3$. Finally, the kinetic model is used to assess the relative importance of the different paths and the extent of amine and thiol assistance.

## RESULTS AND DISCUSSION

Since γ-thiolactones are not symmetric, two sides for nucleophilic attack can be distinguished (Figure 3). These sides are termed *syn* and *anti*, with respect to the position of the equatorial substituent on C2. Conformers where the sub-

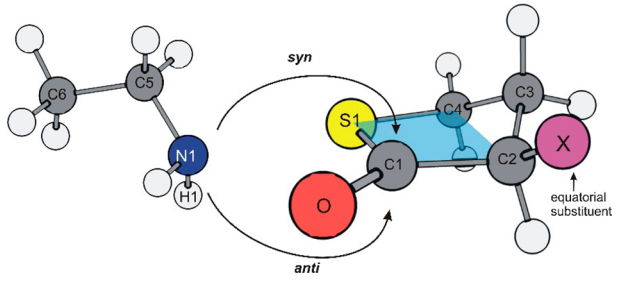


**Figure 3.** *Syn* or *anti* mode of nucleophilic attack at the carbonyl carbon (C1) of a γ-thiolactone.



DOI: 10.1021/acs.joc.5b01446
J. Org. Chem. 2015, 80, 8520−8529

stituent is in axial position are less stable (see section S3 of the Supporting Information).

**Investigation of a Zwitterionic Intermediate.** The existence of the zwitterionic intermediate, ZI in Figure 1, has been investigated for the three selected thiolactones by scanning the structures appearing along the N1−C1 coordinate in steps of 0.1 Å. In Figure 4, the calculated results for γTBL and ActHcy are shown. For γTBL and tHcy (not shown), there is a continuous rise in energy as the N1−C1 distance shortens, until at a distance of 1.4−1.5 Å the C1−S1 bond breaks and a proton transfer occurs between N1 and S1, leading to the ring-opened reaction product. When the COSMO[57] implicit solvation model is applied, the energy rise becomes less pronounced with increasing value of the dielectric constant ($\varepsilon_r$).

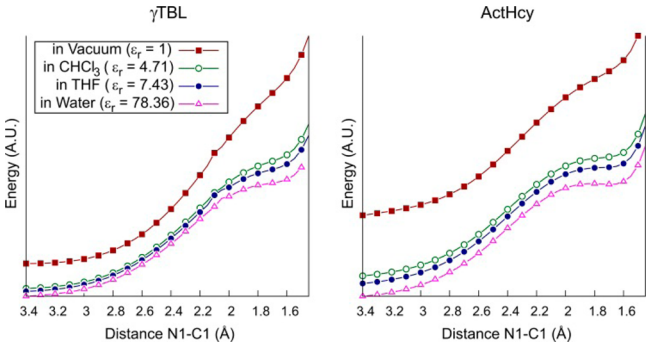


**Figure 4.** Scan along the *anti* N1−C1 coordinate for the reaction of ethylamine with γTBL (left) and ActHcy (right) at the B3LYP/6-311G(2d,d,p) level of theory in vacuum (squares), in $CHCl_3$ (empty circles, $\varepsilon_r$ = 4.71), in THF (filled circles, $\varepsilon_r$ = 7.43), and in water (triangles, $\varepsilon_r$ = 78.36). The zwitterionic intermediate appears as a very shallow local minimum on the potential energy surface for ActHcy when the dielectric constant of the solvent is large enough ($\varepsilon_r$ > 7.43) but not for γTBL.

For the three thiolactones, all attempts to identify a zwitterionic intermediate as a minimum on the potential energy surface in the gas phase failed. Since this paper focuses on a quantitative analysis of the aminolysis in the gas phase and in aprotic media and since zwitterionic species are not reported to be involved in the aminolysis of ester,[44] thioesters,[53] or oxazolinones,[50] it has been opted to defer the study of the stepwise zwitterionic path until later. Hence, in this paper, we choose to follow a uniform approach starting from gas phase calculations to which corrections for solvation are added afterward using COSMO-RS.

**Thermodynamics.** Reaction energies, enthalpies, entropies, and free energies are given in Table 1 for the neutral intermediate and product structures appearing in Figure 1. The aminolysis of the α-substituted thiolactones is more exothermic, which is, however, partially compensated by a higher decrease in entropy, making it only slightly more exergonic. The formation of the tetrahedral intermediates formed in the stepwise mechanism is also exothermic, however, the even bigger loss in entropy makes this an endergonic reaction.

The side of nucleophilic attack, *syn* or *anti*, determines whether in the formed tetrahedral intermediate the incoming amine group is *cis* or *trans* relative to the equatorial substituent X. Note, however, that when X = H, as in the case of γTBL, *syn* or *anti* nucleophilic attack results in different conformers which can interconvert into each other over a lowly activated transition state (18.5 kJ $mol^{-1}$, in vacuum). The intermediate resulting from the *anti* attack has a lower energy and has consequently been used. Solvation only has a minor influence on the reaction thermodynamics. The global reactions become slightly more exothermic by 5−10 kJ $mol^{-1}$ in THF and by 0−5 kJ $mol^{-1}$ in chloroform.

**Concerted Path.** A first possibility for the aminolysis of thiolactones is given by the concerted reaction path, in which creation of the N1−C1 bond, cleavage of the C1−S1 bond, and a proton transfer from N1 to S1 occur simultaneously (Figure 5, *syn*). As discussed previously, there are two possible sides of attack, giving rise to two different transition states, **C**-*syn* and **C**-*anti*, of which the Newman projections are given in Figure 6. All transition state structures and their important geometrical parameters can be found in section S4 of the Supporting Information.

The atomic rearrangement occurring along the concerted path can be monitored closely by following the intrinsic reaction coordinate (IRC) and is shown for γTBL in Figure 7a,b. Similar plots for tHcy and ActHcy can be found in section S4 of the Supporting Information.

Analysis of the geometrical parameters and of the reaction trajectory shows that, regardless of the substituent or the orientation of nucleophilic attack, both the formation of the

**Table 1. Reaction Energies, $\Delta E_r$, Enthalpies, $\Delta H°_r$, Gibbs Free Energies, $\Delta G°_r$ (kJ $mol^{-1}$), and Entropies, $\Delta S_r$ (J $mol^{-1}$ $K^{-1}$), Calculated at the CBS-QB3 Level of Theory for the Products (T) and Neutral Intermediate (NI) Structures Appearing in the Aminolysis of Three γ-Thiolactones with Ethylamine As Shown in Figure 1[a]**

| Product (T) | | gas phase | | | THF | $CHCl_3$ |
|---|---|---|---|---|---|---|
| α-substituent | $\Delta E_r$ | $\Delta H°_r$ | $\Delta S°_r$ | $\Delta G°_r$ | $\Delta G°_r$ | $\Delta G°_r$ |
| H | -56.0 | -56.5 | -159.0 | -25.0 | -36.9 | -31.8 |
| $NH_2$ | -66.4 | -68.6 | -182.1 | -30.2 | -35.4 | -29.1 |
| $NH(CO)CH_3$ | -64.7 | -65.8 | -178.3 | -28.5 | -38.1 | -30.0 |

| Intermediate (NI) | | gas phase | | | | THF | $CHCl_3$ |
|---|---|---|---|---|---|---|---|
| α-substituent | Orientation | $\Delta E_r$ | $\Delta H°_r$ | $\Delta S°_r$ | $\Delta G°_r$ | $\Delta G°_r$ | $\Delta G°_r$ |
| H | - | -10.8 | -15.4 | -213.8 | 32.5 | 20.3 | 30.4 |
| $NH_2$ | *trans* | -15.3 | -19.9 | -214.5 | 28.3 | 15.2 | 25.2 |
| | *cis* | -4.3 | -8.3 | -210.1 | 38.5 | 24.0 | 34.5 |
| $NH(CO)CH_3$ | *trans* | -16.0 | -20.0 | -204.6 | 25.2 | 17.8 | 27.6 |
| | *cis* | -9.9 | -14.7 | -220.6 | 35.3 | 18.9 | 31.1 |

[a]Reaction energies are given at 0 K and contain zero-point vibrational energy corrections. Reaction enthalpies, entropies, and Gibbs free energies are given at 298 K. Reaction Gibbs free energies in THF and $CHCl_3$ are corrected for solvation using COSMO-RS.



DOI: 10.1021/acs.joc.5b01446
J. Org. Chem. 2015, 80, 8520−8529

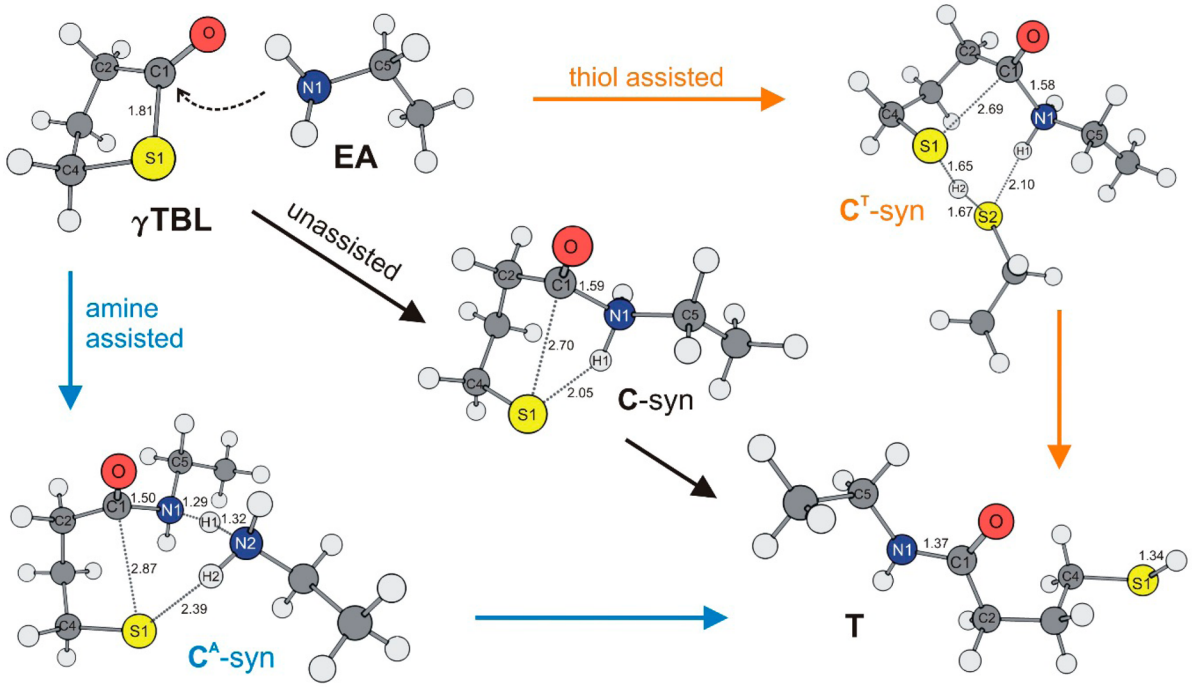


**Figure 5.** B3LYP/6-311G(2d,d,p) optimized geometries of reactants, transition states, and product along the unassisted, amine-assisted, and thiol-assisted concerted path for the aminolysis of γTBL (only *syn* paths shown).

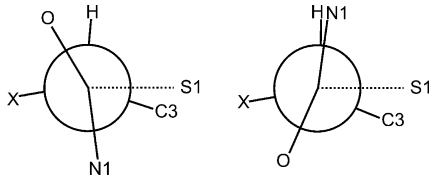


**Figure 6.** Newman projection along the C1 (proximal)−C2 (distal) axis of the transition state for the *syn* (left) and *anti* (right) attack in the concerted path.

N1−C1 bond (1.5−1.6 Å) and the rupture of the C1−S1 (2.7−2.9 Å) bond are substantially advanced in the transition state. The N1−H1 bond (1.1 Å) on the other hand is only very slightly elongated, indicating that proton transfer still has to take place. Furthermore, the reaction trajectory also shows that the formation of the N1−C1 bond and the scission of the C1−S1 bond occur gradually and simultaneously, while the elongation of the N1−H1 and the shortening of the H1−S1 distances occur more abruptly along the reaction coordinate. The reaction profile clearly illustrates that the concerted path is characterized by asynchronous bond breaking and formation.

In the transition states of tHcy and ActHcy, there is the additional possibility of internal hydrogen bonding between the amine proton of the attacking nucleophile amine and a hydrogen bond acceptor on the substituent (N for tHcy and O for ActHcy). For tHcy, this is possible in the *syn* transition state, while for ActHcy, this is possible for both orientations of attack (Figure S1 in section S4 of the Supporting Information). Transition state structures in which hydrogen bonding occurs show slightly more advanced formation of the N1−C1 bond and cleavage of the C1−S1 bond. Analysis of the IRC for these structures (see section S4 of the Supporting Information) reveals additionally that the free energy barrier is lower and less steep.

The concerted path can also occur via an amine-assisted mechanism in which a second amine molecule intervenes in the formation of the transition state (Figure 5). This mechanism involves a double proton transfer over a six-membered ring, which causes less ring strain than in the case of the four-membered ring structure formed in the unassisted mechanism, as has earlier been reported for the aminolysis of esters.[43] Study of the IRC further reveals the nature of this proton shuttle (Figure 7c,d). First, H1 is transferred from N1 of the attacking amine to N2 of the assisting amine, at which point the energy barrier reaches its maximum. Second, a proton from the assisting amine molecule, H2, is transferred from N2 to the sulfur of the thiolactone ring, S1. A direct relationship between the development of the N1−C1 bond and the height of the energy barrier can be observed for the unassisted concerted mechanism. Although the overall reaction profile is quite similar for all three thiolactones, the energy and Gibbs free energy barrier clearly depend on the type of thiolactone. This is mainly related to the possibility of hydrogen bonds being formed in the transition state. In most cases, assistance by either an amine or a thiol significantly reduces the gas phase energy barrier at 0 K, $\Delta E^{\ddagger}$, and much more so for amine assistance than for thiol assistance. However, this effect is much less pronounced for the Gibbs free energy barriers at 298 K, $\Delta G^{\ddagger}$, which, of course, is a consequence of the large entropy penalty due to the involvement of three molecules in the formation of the transition state. In the case of thiol assistance, at 298 K, this entropy penalty even exceeds the decrease in the activation enthalpy $\Delta H^{\ddagger}$, effectively increasing the Gibbs free energy barrier as compared to the unassisted case. In contrast to the thermodynamics of the reactions (Table 1), solvation does have a significant influence on the barrier heights and reduces these on average with 25 kJ mol$^{-1}$ in THF and with 15 kJ mol$^{-1}$ in $CHCl_3$.

In summary, the computational results indicate that, for the concerted path in aprotic media, the amine-assisted mechanism


DOI: 10.1021/acs.joc.5b01446
J. Org. Chem. 2015, 80, 8520−8529

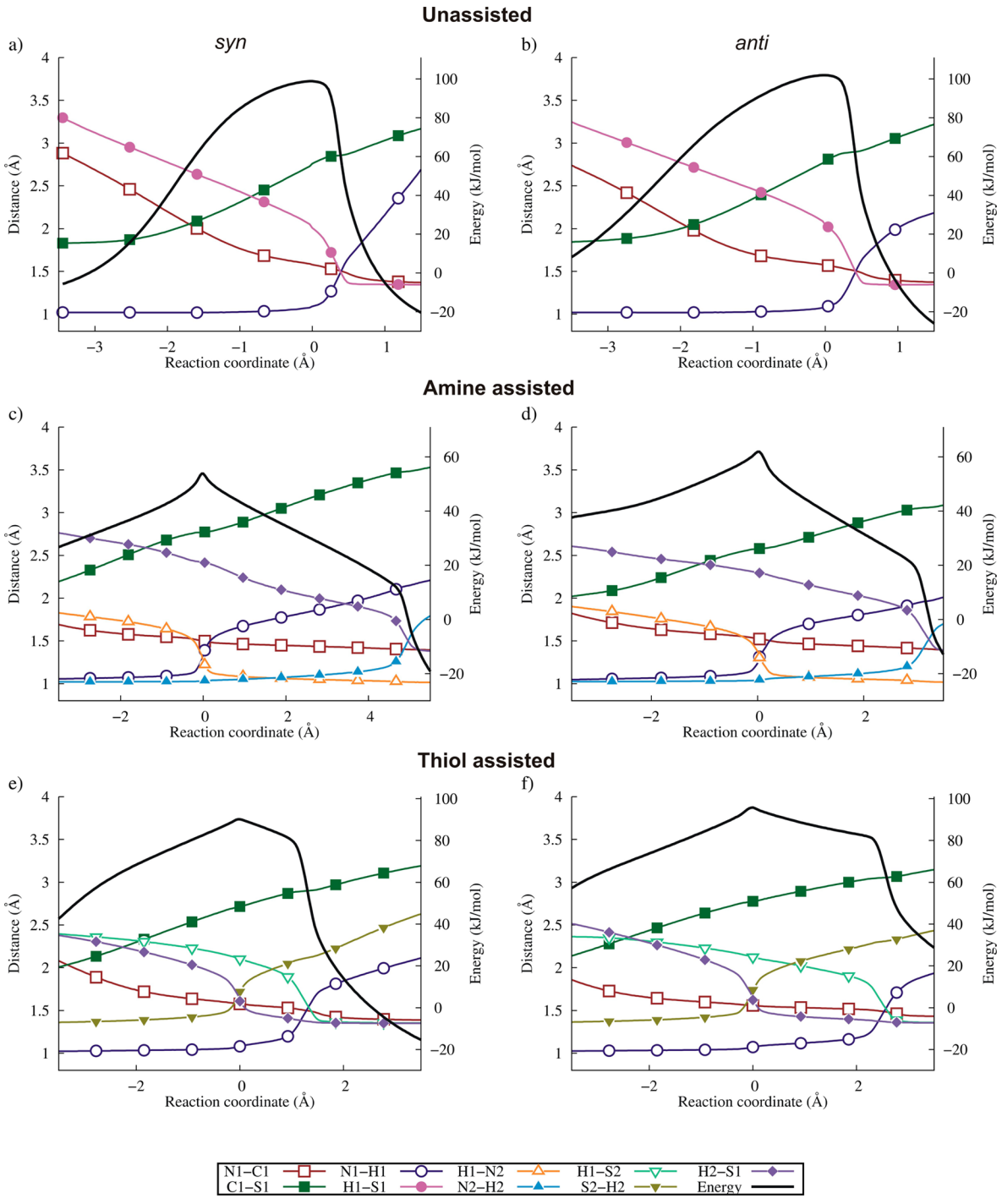


**Figure 7.** Evolution of bond lengths and energy profiles along the intrinsic reaction coordinate for the aminolysis of γTBL with ethylamine via the concerted path. Unassisted: (a) *syn* and (b) *anti*. Amine-assisted: (c) *syn* and (d) *anti*. Thiol-assisted: (e) *syn* and (f) *anti*. Thiol assistance is modeled using ethanethiol as a model for the ring-opened thiolactone. The atom numbering corresponds to Figure 5. A value of 0 in the reaction coordinate (*x*-axis) coincides with the transition state.

is energetically favored over the thiol-assisted and unassisted mechanism. In general, in the concerted mechanisms, the preferred mode of attack of the amine is *anti* relative to the X substituent.

**Neutral Stepwise Pathway.** A second possibility for the aminolysis of thiolactones is given by the neutral stepwise pathway, shown in Figure 8.

This path can be characterized as an addition/elimination reaction.[51] In the first step, the N1−C1 bond is formed and a proton of the attacking amine, H1, is transferred to the carbonyl oxygen O. Likewise, as for the concerted path, there are two possible sides of attack, resulting in a neutral intermediate, NI. In the case of substituted thiolactones, this intermediate can be either *cis* or *trans* in terms of the orientation of the incoming amine with respect to the X substituent. Analysis of the geometrical parameters and the IRC (see section S4 of the Supporting Information) shows that, in the first step, regardless of the substituent or the orientation



DOI: 10.1021/acs.joc.5b01446
J. Org. Chem. 2015, 80, 8520−8529

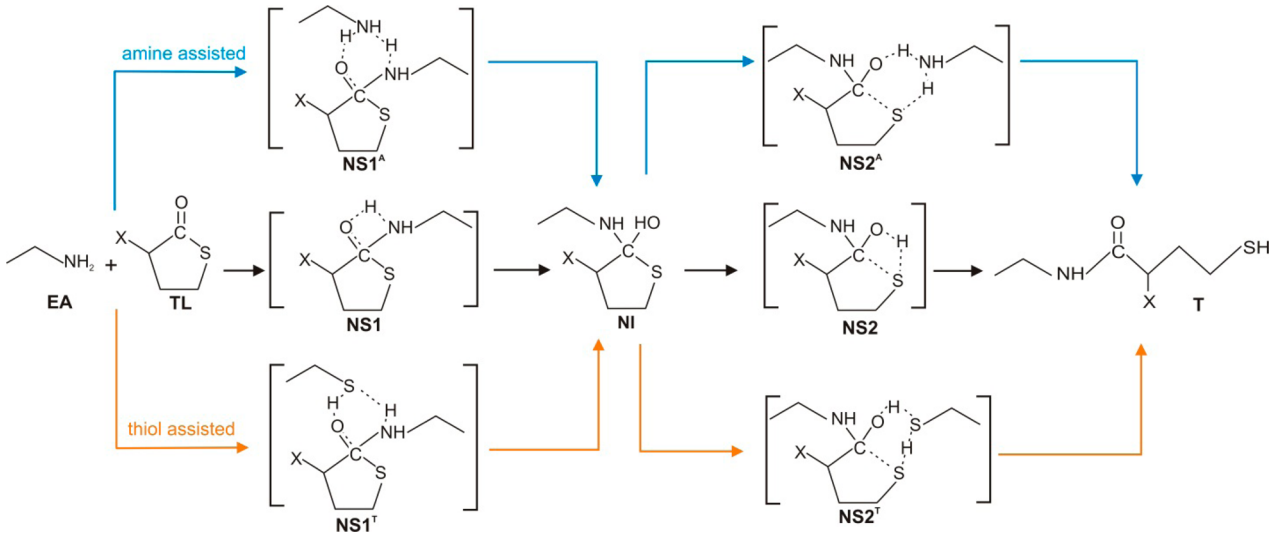


**Figure 8.** Unassisted, amine-assisted, and thiol-assisted mechanism for the neutral stepwise aminolysis of a thiolactone. Thiol assistance is modeled using ethanethiol as a model for the ring-opened thiolactone.

**Table 2. Reaction Barriers at 0 K, $\Delta E^{\ddagger}$, Activation Enthalpies, $\Delta H^{\ddagger}$, Gibbs Free Energy Barriers, $\Delta G^{\ddagger}$ (kJ mol$^{-1}$), and Activation Entropies, $\Delta S^{\ddagger}$ (J mol$^{-1}$ K$^{-1}$), Calculated at the CBS-QB3 Level of Theory for the Concerted and the Neutral Stepwise Path of the Aminolysis of Three γ-Thiolactones with Ethylamine**[a]

| | | | gas phase | | | | | | | | THF | | $CHCl_3$ | |
|---|---|---|---|---|---|---|---|---|---|---|---|---|---|---|
| | | | $\Delta E^{\ddagger}$ (0 K) | | $\Delta H^{\ddagger}$ (298 K) | | $\Delta S^{\ddagger}$ (298 K) | | $\Delta G^{\ddagger}$ (298 K) | | $\Delta G^{\ddagger}$ (298 K) | | $\Delta G^{\ddagger}$ (298 K) | |
| | | reactant | *syn* | *anti* | *syn* | *anti* | *syn* | *anti* | *syn* | *anti* | *syn* | *anti* | *syn* | *anti* |
| | | | | | | | concerted pathway | | | | | | | |
| | unassisted | γTBL | 100.8 | 103.1 | 95.8 | 98 | −213.4 | −212.9 | 143.5 | 145.7 | 116.4 | 118.7 | 126.8 | 129.4 |
| | | tHcy | 87.4 | 120.1 | 82.2 | 115.6 | −214.5 | −207.8 | 130.3 | 161.7 | 113 | 132.8 | 120.2 | 146.3 |
| | | ActHcy | 80.1 | 73.6 | 74.8 | 68.8 | −222.7 | −218.4 | 125.3 | 118.1 | 106 | 100.5 | 116.6 | 110.3 |
| | amine-assisted | γTBL | 48.3 | 50.9 | 42.1 | 44.1 | −387.3 | −400.5 | 125.9 | 131.8 | 99.3 | 107.9 | 103.7 | 117.5 |
| | | tHcy | 46.8 | 34.7 | 40.4 | 27.5 | −393.4 | −407.1 | 126 | 117.1 | 97.0 | 90.3 | 105.8 | 102.5 |
| | | ActHcy | 50.1 | 31.5 | 43.5 | 24.5 | −402.8 | −408.4 | 131.9 | 114.6 | 99.6 | 87.3 | 112.2 | 108.3 |
| | thiol-assisted | γTBL | 76.3 | 65.2 | 70.0 | 58.9 | −395.2 | −395.6 | 156.1 | 145.1 | 127.7 | 115.5 | 143.6 | 131.4 |
| | | tHcy | 63.8 | 62.0 | 57.1 | 55.6 | −399.9 | −397.1 | 144.7 | 142.3 | 125.0 | 123 | 134.9 | 134.4 |
| | | ActHcy | 61.5 | 39.9 | 54.9 | 33.4 | −407.6 | −405.7 | 144.7 | 122.7 | 121.1 | 97.2 | 136.4 | 110 |
| | | | | | | | neutral stepwise pathway | | | | | | | |
| step I | unassisted | γTBL | 142.6 | 137.2 | 137.2 | 132.4 | −219.2 | −209.9 | 186.8 | 179.1 | 175.3 | 163.8 | 174.5 | 164.2 |
| | | tHcy | 114.3 | 127.7 | 108.4 | 122.7 | −226 | −212.4 | 159.9 | 170.2 | 149.7 | 149.1 | 150.4 | 151.9 |
| | | ActHcy | 118.2 | 106.9 | 112.9 | 101.2 | −225.3 | −226.8 | 164.2 | 152.9 | 150.5 | 146.1 | 154.9 | 149.6 |
| | amine-assisted | γTBL | 39.2 | 35.9 | 31.4 | 28.6 | −408.1 | −400.8 | 121.4 | 116.4 | 100.6 | 97.1 | 105.9 | 101.7 |
| | | tHcy | 38.0 | 21.4 | 29.9 | 13.3 | −415.4 | −410.1 | 122 | 103.9 | 102.3 | 88.2 | 111.6 | 94.6 |
| | | ActHcy | 43.3 | 12.6 | 35.4 | 4.9 | −418.1 | −410.2 | 128.4 | 95.5 | 105.2 | 79.8 | 117.8 | 93.2 |
| | thiol-assisted | γTBL | 43.1 | 36.3 | 35.6 | 28.6 | −409.7 | −403.4 | 126 | 117.1 | 96.0 | 92.5 | 101.7 | 105.6 |
| | | tHcy | 34.6 | 25.2 | 26.7 | 17.3 | −411.6 | −408.6 | 117.7 | 107.5 | 94.5 | 86.1 | 106.5 | 97.8 |
| | | ActHcy | 34.6 | 17.4 | 26.8 | 9.7 | −412.6 | −406.9 | 118.1 | 99.3 | 95.0 | 77.8 | 104.8 | 89.4 |
| step II | unassisted | γTBL | 100.0 | 86.9 | 99.5 | 86.3 | 4.3 | 1.82 | 98.2 | 85.8 | 90.0 | 88.6 | 88.7 | 86.6 |
| | | tHcy | 85.2 | 109.2 | 84.2 | 108.9 | 7.4 | 2.54 | 82.0 | 108.2 | 83.1 | 100.1 | 79.4 | 99.7 |
| | | ActHcy | 94.1 | 79.8 | 93.3 | 78.3 | −2.3 | −16.3 | 94.0 | 83.2 | 88.9 | 77.8 | 87.1 | 77.3 |
| | amine-assisted | γTBL | 7.8 | 6.5 | 5.2 | 3.9 | −185.0 | −184.2 | 44.5 | 42.9 | 41.6 | 40.5 | 41.2 | 41.6 |
| | | tHcy | 2.2 | 15.7 | −0.6 | 13.6 | −189.1 | −179.9 | 39.9 | 51.4 | 37.6 | 48.0 | 37.4 | 47.3 |
| | | ActHcy | 16.3 | 4.1 | 14.5 | 1.5 | −176.0 | −185.8 | 51.1 | 41.0 | 46.5 | 25.6 | 48.2 | 28.9 |
| | thiol-assisted | γTBL | 53.3 | 48.2 | 51.5 | 46.3 | −180.9 | −180.3 | 89.5 | 84.2 | 85.0 | 82.8 | 85.4 | 85.7 |
| | | tHcy | 51.5 | 55.3 | 49.1 | 53.5 | −185.8 | −180.1 | 88.6 | 91.3 | 86.2 | 92.2 | 86.4 | 94.4 |
| | | ActHcy | 53.3 | 49.7 | 51.7 | 47.6 | −181.2 | −189.9 | 89.9 | 88.3 | 88.2 | 84.1 | 91.4 | 87.6 |

[a]Reaction barriers at 0 K contain zero-point vibrational energy corrections. Activation enthalpies and Gibbs free energy barriers are given at 298 K. Gibbs free energy barriers in THF and $CHCl_3$ are corrected for solvation using COSMO-RS.

of the nucleophilic attack, the energy maximum coincides with the proton transfer between N1 and O. The formation of the N1−C1 bond occurs gradually, as in the case of the unassisted concerted mechanism. The C1−S1 bond is only slightly



DOI: 10.1021/acs.joc.5b01446
J. Org. Chem. 2015, 80, 8520−8529

stretched, while the C1−O bond lengthens as the double bond character vanishes and the hybridization of C1 and O changes from $sp^2$ to $sp^3$. Similar to the assisted concerted mechanisms, six-membered ring structures can be formed by assistance of an amine or thiol molecule to facilitate the proton transfer. The assisting amine first takes up a proton, H1, from the incoming amine nucleophile before releasing one of its protons, H2, to the carbonyl oxygen, O. The inverse situation is the case when the assisting molecule is a thiol. Both the formation of the N1−C1 bond and the rupture of the C1−S1 bond are not affected significantly.

After formation of the tetrahedral intermediate, a second transition is required to break the C1−S1 bond and move the proton from the carbonyl oxygen to the thiolactone sulfur S1. The geometrical parameters and the IRC (see section S4 of the Supporting Information) indicate that, in the transition states of the unassisted mechanism, cleavage of the C1−S1 bond is already far advanced, while the proton H1 is still present on the carbonyl oxygen. The C1−O double bond character is regained when this second proton transfer takes place. Again, this proton transfer can be assisted by an amine or thiol molecule, which occurs in a similar fashion as already discussed previously.

Gas phase energy barriers at 0 K ($\Delta E^{\ddagger}$), activation enthalpies ($\Delta H^{\circ\ddagger}$), entropies ($\Delta S^{\circ\ddagger}$), and Gibbs free energies ($\Delta G^{\circ\ddagger}$) for the neutral stepwise path are given in Table 2. For the three γ-thiolactones, the second step in this stepwise mechanism is significantly less activated as compared to the first step. The involvement of an amine or a thiol molecule in the stepwise mechanism lowers the energy barrier of the first step to an even larger extent than was the case for the concerted mechanism. Moreover, while for the concerted path assistance by an amine is clearly more effective than by a thiol, this is not the case here, and both types of assistance lower the energy barrier of the first step almost equally. On the other hand, for the second step, assistance by an amine is much more efficient than assistance by a thiol.

Although qualitatively the profiles of the atomic rearrangements, as shown in the IRC plots (see section S4 of the Supporting Information), are similar for all three thiolactones, significant differences in activation barriers can be noticed depending on the substituent as well as on the orientation of attack in those cases, where internal hydrogen bonding becomes possible. Solvation in a polar aprotic solvent affects this stepwise path to a somewhat lesser extent than it does for the concerted path, although the decrease in barrier height is still significant for the first step. The effects of solvation on the second step, however, are only minor due to the structural similarity of the transition state and the intermediate structure.

By comparing the general free energy profiles of the neutral stepwise and the concerted path, some general conclusions can be made, irrespective of the substituent on the thiolactone and the solvent. The free energy barrier of the unassisted concerted mechanism is significantly lower than that for the unassisted neutral stepwise mechanism. However, once assisting molecules come into play, the energetics of the assisted neutral stepwise mechanisms improve dramatically, especially for the first step, and to a much larger extent than for the assisted concerted mechanisms. Apparently, the six-membered ring structures formed for proton transfer are more stable if they involve the carbonyl oxygen O instead of the sulfur S1. Thiol assistance only seems to favor the first step of the stepwise mechanism, and concerted transition states even increase in energy when thiols are involved.

When looking at the difference between *syn* and *anti* attack, the type of thiolactone does play a significant role. For γTBL, differences in orientation are rather small in all mechanisms and usually amount to a value around 5−10 kJ $mol^{-1}$. For tHcy and ActHcy, however, significant differences in reactivity occur as the substituents could both cause steric hindrance as well as open the possibility for hydrogen bond formation. This is especially the case for ActHcy, distinctively lowering its energy barrier as compared to the unsubstituted thiolactone.

**Kinetic Analysis of the Aminolysis of ActHcy.** Envisioning future applications of thiolactones in a macromolecular context, ActHcy is the most interesting model compound due to its substituent being a good model for a urethane bond.[11] To obtain a complete understanding of the reactivity and the relative importance of the different mechanisms, it becomes pertinent to construct a kinetic model. Using the ab initio obtained Gibbs free energies of reaction and Gibbs free energy barriers in both THF and $CHCl_3$, equilibrium coefficients and rate coefficients for all elementary steps as given in Table 2 are calculated at 298.15 K via the standard statistical thermodynamic formulas 2−4:

$$k_f(T) = \frac{k_B T}{h} e^{-\Delta G^{\ddagger}/RT} \quad (2)$$

$$K(T) = e^{-\Delta G_r/RT} \quad (3)$$

$$k_b = \frac{k_f(T)}{K(T)} \quad (4)$$

where $K$, $k_f$, and $k_b$ are the equilibrium, the forward rate, and the backward rate coefficient, respectively, for the appropriate elementary step.

Conversion profiles of the aminolysis of ActHcy with *n*-butylamine in a range of initial conditions (see Table 3) are monitored using online FTIR and GC, in both THF and $CHCl_3$. It has been verified that the calculated thermodynamic and kinetic parameters for ethylamine and *n*-butylamine are very similar (see section S5 of the Supporting Information).

**Table 3. Overview of Initial Reaction Conditions Used for the Aminolysis of ActHcy with *n*-Butylamine**

| entry | $[ActHcy]_0$ (M) | $[n\text{-butylamine}]_0$ (M) | solvent |
|---|---|---|---|
| 1 | 1.0 | 0.5 | $CHCl_3$ |
| 2 | 1.0 | 1.0 | $CHCl_3$ |
| 3 | 1.0 | 1.5 | $CHCl_3$ |
| 4 | 0.5 | 0.55 | THF |
| 5 | 0.5 | 0.75 | THF |
| 6 | 0.5 | 1.0 | THF |
| 7 | 0.1 | 0.1 | THF |
| 8 | 0.1 | 0.15 | THF |

Nevertheless, preliminary results from the kinetic simulations using the ab initio calculated rate coefficients show small systematic discrepancies with the experimental data. This can be rationalized by the fact that (i) ethanethiol is used in the ab initio calculations as a model compound instead of the ring-opened ActHcy, and (ii) although both CBS-QB3 and COSMO-RS are among the most accurate computational methods available, deviations with experimental values on the order of a few kJ $mol^{-1}$ are still possible.[58] Therefore, to allow comparison of the simulated conversion profiles obtained with the experimentally obtained ones, the Gibbs free reaction



DOI: 10.1021/acs.joc.5b01446
J. Org. Chem. 2015, 80, 8520−8529

energy barriers, $\Delta G^{\ddagger}$, of all reaction steps are adjusted in THF with +6 kJ mol$^{-1}$ and in $CHCl_3$ with −3 kJ mol$^{-1}$. Figure 9 shows the results of the simulations using this approach versus the experimental data for different initial conditions.

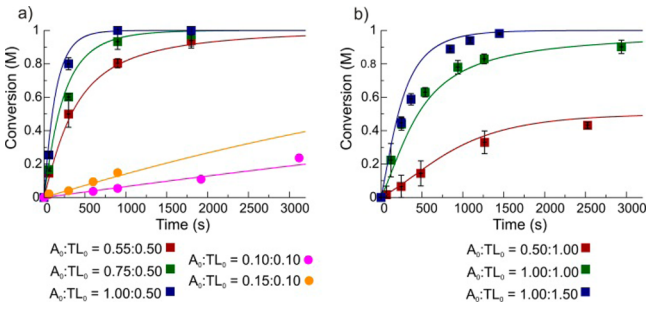


**Figure 9.** Conversion profiles for the aminolysis of ActHcy with *n*-butylamine in THF and in $CHCl_3$ in a range of initial amine to thiolactone ratios ($A_0/TL_0$). Experimental points are given for the aminolysis of ActHcy by *n*-butylamine at 298 K (squares = FTIR, circles = GC). The lines represent the simulation results with the kinetic model parameters based on the ab initio data (see text).

Having established the validity of the kinetic model in a range of conditions, it can now be used to get more insight into the mechanism of the aminolysis. As discussed previously, for the unassisted mechanisms, the concerted path is energetically favored over the neutral stepwise path, while for both the amine- and thiol-assisted case, the stepwise path is the energetically preferred route. The fractional contributions of each mechanism to the total conversion of ActHcy in both THF and $CHCl_3$ are provided in section S6 of the Supporting Information for a range of conditions relevant for applications in polymer chemistry.[11] In Figure 10, the main fractional contributions for the principally occurring mechanisms to the aminolysis of ActHcy in THF are shown.

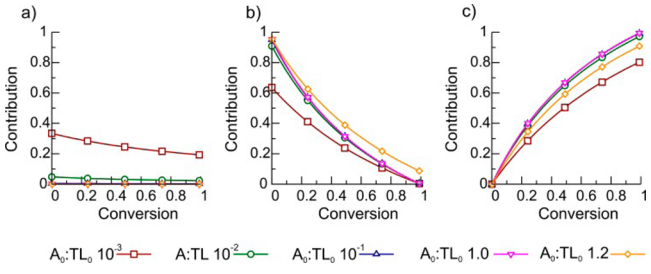


**Figure 10.** Fractional contributions to the conversion in a range of initial amine to thiolactone ratios ($A_0$:$TL_0$) of the main contributing mechanisms to the aminolysis of 0.5 M ActHcy in THF: the unassisted concerted mechanism (left), the amine-assisted stepwise mechanism (middle), and the thiol-assisted stepwise mechanism (right). Fractional contributions to the conversion for the other mechanisms in THF and in $CHCl_3$ are given in section S6 of the Supporting Information.

Clearly, at low thiolactone conversion, aminolysis preferentially occurs via the amine-assisted stepwise mechanism while the thiol-assisted stepwise mechanism gradually takes over as the reaction progresses and the thiol concentration in the reaction mixture steadily increases. Note that for both the amine- and thiol-assisted stepwise mechanisms, there is an overwhelming preference for *anti* attack (see Figure S9 in section S6 of the Supporting Information), implying a stereoselective ring opening of ActHcy. The unassisted concerted mechanism only starts to contribute significantly when the initial amine concentration is some hundred times smaller than the initial thiolactone concentration. This is the case both in THF and in $CHCl_3$ (see Figures S8 and S11 in section S6 of the Supporting Information), although in $CHCl_3$, the contribution from the unassisted reaction mechanism is higher than that in THF for similar conditions. Note that the ratios in which the amine- and thiol-assisted mechanisms contribute depend on the solvent because the difference in free energy barrier between the thiol- and amine-assisted transition state might vary in different solvents. Furthermore, in the stepwise path, the formation of the intermediate is rate-determining, as is evidenced by the much greater affinity,[59] shown in section S7 of the Supporting Information.

In summary, the kinetic analysis clearly reveals that, in practically relevant reaction conditions, the contribution of the thiol-assisted stepwise mechanism is substantial while the unassisted concerted mechanism can be safely ignored. Hence, it can be concluded that rate laws of the form of eq 1 will not be able to provide an adequate description of the aminolysis of thiolactones in reaction conditions relevant for applications in polymer chemistry, and instead, a rate law in the form of eq 5 is proposed:

$$r_{obs} = k_1[\text{amine}]^2[\text{thiolactone}] + k_2[\text{amine}][\text{thiolactone}][\text{thiol}] \quad (5)$$

where $k_1$ and $k_2$ are the observed apparent rate coefficients. The first term corresponds to the amine-assisted path and the second to the thiol-assisted path.

## CONCLUSIONS

The aminolysis of $\gamma$-thiolactones is investigated via ab initio calculations at the CBS-QB3 level. The first quantitative theoretical results are provided for the two competing reaction paths, a concerted and a neutral stepwise path. The involvement of proton transfer in both paths is crucial in determining the height of the reaction barrier. This barrier is lowered significantly via assistance by another amine or by the formed thiol. Both forms of assistance are characterized by the introduction of an additional proton transfer and differ in the order of the proton transfers: the assisting amine first accepts a proton from the incoming amine before donating one of its protons to the thiolactone sulfur, while the thiol first donates its proton before accepting one from the incoming amine. Especially, the first step of the neutral stepwise mechanism is favored by this assistance and, while hugely unfavorable in the unassisted case, becomes the dominant mechanism. The presence of aprotic solvents, such as THF or $CHCl_3$, has been modeled using COSMO-RS and substantially lowers the Gibbs free energy barriers along all paths.

A kinetic model is constructed using the CSB-QB3 calculated thermodynamic and kinetic parameters, which are corrected for solvation using COSMO-RS and adjusted slightly, well within the margin of computational error, to match experimental data. The presented kinetic model helps to understand the role of the assisting amine and thiol molecules during the reaction. It is demonstrated that the unassisted concerted mechanism only significantly contributes in the case of very low amine concentrations and that it can safely be ignored in the practically relevant case of (quasi-)equimolar initial concentrations of amine and thiolactone. However, under the latter practical conditions, the contribution of thiol assistance to the


DOI: 10.1021/acs.joc.5b01446
J. Org. Chem. 2015, 80, 8520−8529

total thiolactone conversion is significant and cannot be ignored.

Both the ab initio and kinetic modeling results provide a theoretical framework to fundamentally understand the different factors determining the reaction kinetics of the aminolysis of γ-thiolactones, which is vital for their further application as thiol precursors in, for instance, polymerization.

## EXPERIMENTAL SECTION

**Computational Methods.** All of the electronic structure calculations are performed using the Gaussian 09 package.[60] Global minimum energy conformations for reactants, products, and intermediates are determined in vacuo by a first thorough scan of all freely rotating dihedral angles at the HF/6-31G(d) level of theory followed by a further scanning at the B3LYP/6-31G(d) level of theory of the conformers, which were within a 25 kJ $mol^{-1}$ bracket of the lowest energy conformer, after which a full geometry optimization and free energy calculation are performed using the CBS-QB3 composite method.[55] All thermal contributions were calculated in the harmonic oscillator approach. For the optimization of transition states, the Berny algorithm is applied.[61] Minimum energy conformations and transition states are confirmed to have zero and one imaginary frequency, respectively. Additionally, the reaction trajectory path has been monitored by following the intrinsic reaction rate at the B3LYP/6-31G(d) level of theory. Correction terms for solvation are calculated using COSMO-RS[56] theory as implemented in the COSMOtherm[62] software. The input structures for COSMOtherm are calculated by Gaussian using the SCRF=COSMORS keyword, based on the B3LYP/6-311G(2d,d,p) optimized structures, which are recalculated at the BP86/TZVP level of theory, for which COSMOtherm is parametrized. Solvent models for THF and chloroform are used as implemented in the COSMOtherm software. All enthalpies, entropies, and free energies are calculated with respect to a standard state of 1 mol/L. Note that free energies in solution cannot be split up in terms of enthalpy and entropy due to the degree of parametrization present. Additionally, for the identification of stable zwitterionic species, scans along the N−C reaction coordinate are carried out at the B3LYP/6-311G(2d,d,p) level of theory in conjunction with an implicit solvation model, COSMO[57] (COnductor like Screening MOdel), which is termed C-PCM[63] in the Gaussian 09 package, using the parametrized values for $CHCl_3$, THF, and water as implemented in the model.

**Kinetic Model.** A reaction scheme containing all the elementary steps for the concerted and stepwise paths, both unassisted and assisted, has been considered. For each elementary step, the forward and backward rates are calculated based on the ab initio calculated rate coefficients. Integration of the continuity equations was performed using the DASPK algorithm, implemented as a double-precision Fortran code (DDASPK). This code uses backward differentiation formulas and is based on the integration methods of the solver DASSL (differential-algebraic system solver), combined with preconditioned Krylov methods for solving the linear systems at each time step.[64] The selectivity for each reaction mechanism is recorded explicitly during the simulations to allow assessment of the relative contribution to the total rate of reaction.

**Experimental Methods.** *N*-Acetyl-DL-homocysteine thiolactone (ActHcy, >99% pure), *n*-butylamine (99.5% pure), and the solvents tetrahydrofuran (99.9% pure) and chloroform (>99.8% pure) were used as received from a commercial supplier. The aminolysis reaction of ActHcy with *n*-butylamine is monitored using online Fourier transform infrared (FTIR, Mettler Toledo ReactIR 4000), and conversion profiles are obtained by deconvolution of the C=O stretch vibration band (1650−1750 $cm^{-1}$; see section S1 of the Supporting Information). Gas chromatography (see section S2 of the Supporting Information) is used for concentrations too low to follow with FTIR (<0.5 M). The initial experimental conditions are summarized in Table 3.

## ASSOCIATED CONTENT

### Supporting Information

The Supporting Information is available free of charge on the ACS Publications website at DOI: 10.1021/acs.joc.5b01446.

Details of the FTIR deconvolution procedure; GC analysis procedure; computational results on the interconversion of thiolactones; further geometrical details, IRC plots and plots of optimized B3LYP/6-311G(2d,d,p) structures; validation of the use of ethylamine as a model compound for *n*-butylamine in ab initio calculations; relative contributions to the total rate for all mechanisms in THF and $CHCl_3$; Cartesian coordinates of all stationary points reported in this paper and, in the case of saddle points, with their imaginary frequency (PDF)

## AUTHOR INFORMATION


### Corresponding Authors

*E-mail: pieter.espeel@ugent.be.

*E-mail: mariefrancoise.reyniers@ugent.be.


### Notes

The authors declare no competing financial interest.

## ACKNOWLEDGMENTS

The authors acknowledge financial support from the Long Term Structural Methusalem Funding by the Flemish Government, the Interuniversity Attraction Poles Programme, Belgian State−Belgian Science Policy, and the Fund for Scientific Research Flanders (FWO: G045212N). D.R.D. acknowledges the FWO through a postdoctoral fellowship. The computational work was carried out using the STEVIN Supercomputer Infrastructure at Ghent University, funded by Ghent University, the Flemish Supercomputer Center (VSC), the Hercules Foundation and the Flemish Government, department EWI.

## REFERENCES


(1) Garel, J.; Tawfik, D. S. *Chem. - Eur. J.* **2006**, *12*, 4144.

(2) Arora, B.; Narayanasamy, A.; Nirmal, J.; Halder, N.; Patnaik, S.; Ravi, A. K.; Velpandian, T. *J. Chromatogr. B: Anal. Technol. Biomed. Life Sci.* **2014**, *944*, 49.

(3) Clarke, R.; Daly, L.; Robinson, K.; Naughten, E.; Cahalane, S.; Fowler, B.; Graham, I. *N. Engl. J. Med.* **1991**, *324*, 1149.

(4) Najib, S.; Sanchez-Margalet, V. *J. Mol. Endocrinol.* **2001**, *27*, 85.

(5) Jakubowski, H. *Cell. Mol. Life Sci.* **2004**, *61*, 470.

(6) Jalili, S.; Yousefi, R.; Papari, M.-M.; Moosavi-Movahedi, A. *Protein J.* **2011**, *30*, 299.

(7) Ferraris, D. V.; Majer, P.; Ni, C. Y.; Slusher, C. E.; Rais, R.; Wu, Y.; Wozniak, K. M.; Alt, J.; Rojas, C.; Slusher, B. S.; Tsukamoto, T. *J. Med. Chem.* **2014**, *57*, 243.

(8) Benesch, R.; Benesch, R. E. *Proc. Natl. Acad. Sci. U. S. A.* **1958**, *44*, 848.

(9) Benesch, R.; Benesch, R. E. *J. Am. Chem. Soc.* **1956**, *78*, 1597.

(10) Yan, J.-J.; Sun, J.-T.; You, Y.-Z.; Wu, D.-C.; Hong, C.-Y. *Sci. Rep.* **2013**, *3*, 2841.

(11) Espeel, P.; Goethals, F.; Driessen, F.; Nguyen, L.-T. T.; Du Prez, F. E. *Polym. Chem.* **2013**, *4*, 2449.

(12) Yan, J.-J.; Wang, D.; Wu, D.-C.; You, Y.-Z. *Chem. Commun.* **2013**, *49*, 6057.

(13) Keul, H.; Mommer, S.; Möller, M. *Eur. Polym. J.* **2013**, *49*, 853.

(14) Mommer, S.; Keul, H.; Möller, M. *Macromol. Rapid Commun.* **2014**, *35*, 1986.

(15) Goethals, F.; Martens, S.; Espeel, P.; van den Berg, O.; Du Prez, F. E. *Macromolecules* **2014**, *47*, 61.




DOI: 10.1021/acs.joc.5b01446
*J. Org. Chem.* 2015, 80, 8520−8529

(16) Espeel, P.; Goethals, F.; Du Prez, F. E. *J. Am. Chem. Soc.* **2011**, *133*, 1678.
(17) Espeel, P.; Du Prez, F. E. *Eur. Polym. J.* **2015**, *62*, 247.
(18) Espeel, P.; Goethals, F.; Stamenovic, M. M.; Petton, L.; Du Prez, F. E. *Polym. Chem.* **2012**, *3*, 1007.
(19) Belbekhouche, S.; Reinicke, S.; Espeel, P.; Du Prez, F. E.; Eloy, P.; Dupont-Gillain, C.; Jonas, A. M.; Demoustier-Champagne, S.; Glinel, K. *ACS Appl. Mater. Interfaces* **2014**, *6*, 22457.
(20) Chen, Y.; Espeel, P.; Reinicke, S.; Du Prez, F. E.; Stenzel, M. H. *Macromol. Rapid Commun.* **2014**, *35*, 1128.
(21) Reinicke, S.; Espeel, P.; Stamenovic, M. M.; Du Prez, F. E. *Polym. Chem.* **2014**, *5*, 5461.
(22) Espeel, P.; Carrette, L. L. G.; Bury, K.; Capenberghs, S.; Martins, J. C.; Du Prez, F. E.; Madder, A. *Angew. Chem., Int. Ed.* **2013**, *52*, 13261.
(23) Reinicke, S.; Espeel, P.; Stamenović, M. M.; Du Prez, F. E. *ACS Macro Lett.* **2013**, *2*, 539.
(24) Stamenovic, M. M.; Espeel, P.; Baba, E.; Yamamoto, T.; Tezuka, Y.; Du Prez, F. E. *Polym. Chem.* **2013**, *4*, 184.
(25) Espeel, P.; Du Prez, F. E. *Macromolecules* **2015**, *48*, 2.
(26) Beltowski, J. *Postepy Hig. Med. Dosw.* **2005**, *59*, 392.
(27) Hoyle, C. E.; Bowman, C. N. *Angew. Chem., Int. Ed.* **2010**, *49*, 1540.
(28) Yoon, J. A.; Kamada, J.; Koynov, K.; Mohin, J.; Nicolaÿ, R.; Zhang, Y.; Balazs, A. C.; Kowalewski, T.; Matyjaszewski, K. *Macromolecules* **2012**, *45*, 142.
(29) Ghosh, S.; Basu, S.; Thayumanavan, S. *Macromolecules* **2006**, *39*, 5595.
(30) Campos, L. M.; Meinel, I.; Guino, R. G.; Schierhorn, M.; Gupta, N.; Stucky, G. D.; Hawker, C. J. *Adv. Mater.* **2008**, *20*, 3728.
(31) Yuan, Y. C.; Rong, M. Z.; Zhang, M. Q.; Chen, J.; Yang, G. C.; Li, X. M. *Macromolecules* **2008**, *41*, 5197.
(32) Fu, Y.; Kao, W. Y. J. *J. Biomed. Mater. Res., Part A* **2011**, *98A*, 201.
(33) Wong, L.; Boyer, C.; Jia, Z.; Zareie, H. M.; Davis, T. P.; Bulmus, V. *Biomacromolecules* **2008**, *9*, 1934.
(34) Hoogenboom, R. *Angew. Chem., Int. Ed.* **2010**, *49*, 3415.
(35) De, S.; Khan, A. *Chem. Commun.* **2012**, *48*, 3130.
(36) Northrop, B. H.; Coffey, R. N. *J. Am. Chem. Soc.* **2012**, *134*, 13804.
(37) Stolz, R. M.; Northrop, B. H. *J. Org. Chem.* **2013**, *78*, 8105.
(38) Nair, D. P.; Podgorski, M.; Chatani, S.; Gong, T.; Xi, W. X.; Fenoli, C. R.; Bowman, C. N. *Chem. Mater.* **2014**, *26*, 724.
(39) Derboven, P.; D'hooge, D. R.; Stamenovic, M. M.; Espeel, P.; Marin, G. B.; Du Prez, F. E.; Reyniers, M.-F. *Macromolecules* **2013**, *46*, 1732.
(40) Satterthwait, A. C.; Jencks, W. P. *J. Am. Chem. Soc.* **1974**, *96*, 7018.
(41) Menger, F. M.; Smith, J. H. *J. Am. Chem. Soc.* **1972**, *94*, 3824.
(42) Zipse, H.; Wang, L.-H.; Houk, K. N. *Liebigs Annalen* **1996**, *1996*, 1511.
(43) Wang, L.-H.; Zipse, H. *Liebigs Annalen* **1996**, *1996*, 1501.
(44) Ilieva, S.; Galabov, B.; Musaev, D. G.; Morokuma, K.; Schaefer, H. F., 3rd *J. Org. Chem.* **2003**, *68*, 1496.
(45) Rao, H.-B.; Wang, Y.-Y.; Zeng, X.-Y.; Xue, Y.; Li, Z.-R. *Comput. Theor. Chem.* **2013**, *1008*, 8.
(46) Liu, X.-Q.; Jin, L.; Kim, C. K.; Xue, Y. *J. Mol. Catal. A: Chem.* **2012**, *355*, 102.
(47) Jin, L.; Xue, Y.; Zhang, H.; Kim, C. K.; Xie, D. Q.; Yan, G. S. *J. Phys. Chem. A* **2008**, *112*, 4501.
(48) Pocker, Y.; Green, E. *J. Am. Chem. Soc.* **1976**, *98*, 6197.
(49) Mandal, D.; Sen, K.; Das, A. K. *J. Phys. Chem. A* **2012**, *116*, 8382.
(50) Ilieva, S.; Galabov, B.; Musaev, D. G.; Morokuma, K. *J. Org. Chem.* **2003**, *68*, 3406.
(51) Petrova, T.; Okovytyy, S.; Gorb, L.; Leszczynski, J. *J. Phys. Chem. A* **2008**, *112*, 5224.
(52) Castro, E. A. *Pure Appl. Chem.* **2009**, *81*, 685.
(53) Yang, W.; Drueckhammer, D. G. *Org. Lett.* **2000**, *2*, 4133.
(54) Jencks, W. P.; Gilchrist, M. *J. Am. Chem. Soc.* **1968**, *90*, 2622.
(55) Montgomery, J. A.; Frisch, M. J.; Ochterski, J. W.; Petersson, G. A. *J. Chem. Phys.* **1999**, *110*, 2822.
(56) Klamt, A.; Eckert, F. *Fluid Phase Equilib.* **2000**, *172*, 43.
(57) Klamt, A.; Schuurmann, G. *J. Chem. Soc., Perkin Trans. 2* **1993**, 799.
(58) Deglmann, P.; Müller, I.; Becker, F.; Schäfer, A.; Hungenberg, K.-D.; Weiß, H. *Macromol. React. Eng.* **2009**, *3*, 496.
(59) Fishtik, I.; Datta, R. *Ind. Eng. Chem. Res.* **2001**, *40*, 2416.
(60) Frisch, M. J.; Trucks, G. W.; Schlegel, H. B.; Scuseria, G. E.; Robb, M. A.; Cheeseman, J. R.; Scalmani, G.; Barone, V.; Mennucci, B.; Petersson, G. A.; Nakatsuji, H.; Caricato, M.; Li, X.; Hratchian, H. P.; Izmaylov, A. F.; Bloino, J.; Zheng, G.; Sonnenberg, J. L.; Hada, M.; Ehara, M.; Toyota, K.; Fukuda, R.; Hasegawa, J.; Ishida, M.; Nakajima, T.; Honda, Y.; Kitao, O.; Nakai, H.; Vreven, T.; Montgomery, J. A.; Peralta, J. E.; Ogliaro, F.; Bearpark, M.; Heyd, J. J.; Brothers, E.; Kudin, K. N.; Staroverov, V. N.; Kobayashi, R.; Normand, J.; Raghavachari, K.; Rendell, A.; Burant, J. C.; Iyengar, S. S.; Tomasi, J.; Cossi, M.; Rega, N.; Millam, J. M.; Klene, M.; Knox, J. E.; Cross, J. B.; Bakken, V.; Adamo, C.; Jaramillo, J.; Gomperts, R.; Stratmann, R. E.; Yazyev, O.; Austin, A. J.; Cammi, R.; Pomelli, C.; Ochterski, J. W.; Martin, R. L.; Morokuma, K.; Zakrzewski, V. G.; Voth, G. A.; Salvador, P.; Dannenberg, J. J.; Dapprich, S.; Daniels, A. D.; Farkas, Ö; Foresman, J. B.; Ortiz, J. V.; Cioslowski, J.; Fox, D. J. *Gaussian 09*; Gaussian, Inc.: Wallingford, CT, 2009.
(61) Schlegel, H. B. *J. Comput. Chem.* **1982**, *3*, 214.
(62) Diedenhofen, M.; Hellweg, A.; Huniar, U.; Klamt, A.; Loschen, C.; Reinisch, J.; Schroer, A.; Steffen, C.; Thomas, K.; Wichmann, K.; Ikeda, H. *COSMOtherm*; COSMOlogic GmbH & Co. KG: Leverkusen, Germany, 2013.
(63) Barone, V.; Cossi, M. *J. Phys. Chem. A* **1998**, *102*, 1995.
(64) Brown, P. N.; Hindmarsh, A. C.; Petzold, L. R. *Siam J. Sci. Comput.* **1994**, *15*, 1467.


DOI: 10.1021/acs.joc.5b01446
*J. Org. Chem.* 2015, 80, 8520−8529